

The chiral logs of the $K \rightarrow \pi\pi$ amplitude

M. Büchler^a

^a Department of Physics, University of Washington
Seattle, WA 98195-1560, U.S.A.

May 11, 2019

Abstract

I calculate the leading logarithmic contributions up to two-loop order of the octet part of the $K^0 \rightarrow \pi\pi$ amplitude. This sector of the weak chiral Lagrangian is believed to be the main source of the enhancement of the $I = 0$ relative to the $I = 2$ $K^0 \rightarrow \pi\pi$ amplitude, the so-called $\Delta I = 1/2$ rule. I discuss the procedure of chiral extrapolations of lattice data specific to $K \rightarrow \pi\pi$ decays and study the implication of the present calculation on these numerically. The latter reinforces the fact that one has to expect a large enhancement of the $I = 0$ part of the amplitude due to re-scattering effects between the three mesons.

1 Introduction

Chiral logs are introduced during the process of renormalization [1]; In the framework of dimensional regularization, one has to introduce an energy scale ν to ensure the correct dimension of observables: Terms like the one on the LHS of Eq. (1.1), generated by loop integrals in $d = 4 - \varepsilon$ dimensions, are re-expressed in the ν independent form on the RHS¹. It is necessary to adopt the energy scale ν to provide the proper dimension of the divergent and finite pieces in a well-defined way. Physically, the emerging chiral logs can be associated with the infrared singularities when the masses of the theory approach zero,

$$\left(\frac{m^{-\varepsilon}}{\varepsilon}\right)^n \rightarrow \left(\nu^{-\varepsilon}\left(\frac{1}{\varepsilon} - \frac{1}{2}\ln\left(\frac{m^2}{\nu^2}\right)\right)\right)^n, \quad (1.1)$$

and can produce sizeable contributions to amplitudes.

Chiral logarithms are an important ingredient in a lattice determination of the $K^0 \rightarrow \pi\pi$ amplitude: the lattice community commonly uses a standard method to relate the latter to the $K^0 \rightarrow \pi^0$ and $K^0 \rightarrow |0\rangle$ matrix element [2]. However, this approach cannot

¹These terms are multiplied by geometrical factors and polynomials of integer powers in the masses.

account for QCD interactions between the mesons, in particular the so called final state interactions between the two pions. These effects, though, are expected (at least partially) to explain the enhancement of the amplitude with the two pions in the $I = 0$ state relative to the $I = 2$ state ($\Delta = 1/2$ rule) as well as the disagreement of the value of ε'/ε between theory and measurement. CHPT provides a tool to estimate the effects caused by these interactions, and the chiral logs are a numerically important part thereof.

In two flavor CHPT, these contributions are commonly the dominant part of the NNLO corrections, which is illustrated in the case of $\pi\pi$ scattering in [3]. In the case of three flavor CHPT, the double log contributions are however not as prominent. Table 1 shows the chiral corrections up to NNLO to the pion and Kaon decay constants and the vector form factor of K_{l3} [4, 5, 6]. The double logs amount to 20 – 35% of the NNLO order result, corresponding to around 10% of the total corrections at NNLO to the leading order result. Since the latter are of importance in the procedure of the chiral extrapolation discussed later, the double logs can make a sizeable contribution for such applications. In

	LO	NLO	NNLO	Double Logs
F_π/F_0	1	0.068	-0.172	-0.050
F_K/F_π	1	0.216	0.035	0.06
$f_+(0)[K_{l3}]$	1	-0.023	0.015	0.004

Table 1: The chiral corrections up to NNLO for the pion and Kaon decay constants and the vector form factor of K_{l3} . The values can however vary considerably, depending on the LEC's one employs. The numbers above are calculated with some standard values of the NLO LEC's and all the renormalized NNLO LEC's set to zero at $\mu = 770\text{MeV}$.

the framework of CHPT, the interactions between the mesons are encoded in the higher order contributions of the amplitude. So far these contributions can't be determined exactly, since the low energy constants (LEC's) of the weak chiral Lagrangians at \hbar -order 1 (NLO) are not known, let alone the NNLO LEC's. The determination of the leading log contributions is thus the only possibility to get an estimate of the corrections one has to expect at NLO and NNLO. In [7] a method has been proposed to provide the LEC's needed for the $K \rightarrow \pi\pi$ amplitude from lattice simulations.

The outline of the paper is as follows:

In section 2 I introduce some notation and the chiral Lagrangians used in the calculation. Section 3 discusses the procedure of the chiral extrapolation used in lattice determinations of the $K^0 \rightarrow \pi\pi$ amplitude: The quantity which can be extracted from a lattice simulation corresponds to the chiral limit of the amplitude, or, more accurately, the reduced counterpart thereof. In a further step, the obtained chiral limit value has to be transformed back to the physical world with non-vanishing quark masses, which in the context of CHPT corresponds to the re-introduction of interactions between the mesons (i.e. final state interactions), whose importance has already been pointed out.

This step and the numerics thereof are discussed in section 4 at NLO accuracy, emphasizing the role of the chiral logs involved. In section 5 the procedure is extended to include

the double log contributions of this extrapolation, being part of the NNLO corrections to the NLO results of section 4.

In the appendices I outline the more technical aspects of the paper:

Appendix A provides a thorough discussion of the NLO contributions and its approximation using only the chiral logs. Appendix B presents the procedure used to compute the double log contributions of the $K \rightarrow \pi\pi$ amplitude. The double logs are split into different classes of contribution: The "genuine" double logs originating from one particle irreducible (1PI) two loop topologies, which can be calculated with the NNLO counterterm Lagrangian provided in [8]. For a second class, the one particle reducible topologies, one can employ separate one loop calculations for the respective 1PI subgraphs. The results of the needed one loop expressions are given in appendix C. The last contribution originates from lower order diagrams where the masses and decay constants are shifted to their physical value, as well as corrections coming from the wave-function renormalization and LSZ procedure, up to the required chiral order. The mass and decay shifts are provided in appendix D. Appendix E gives a very brief summary of the loop integrals used in appendix C.

2 CHPT Lagrangian

Here I provide a very brief introduction of the Lagrangians which were used in the calculation. For more details about CHPT and in particular the definitions of the building blocks used throughout the paper I refer to the numerous review articles, for instance [9, 10]. The lowest order chiral Lagrangian which allows for $\Delta S = 1$ strangeness changing interactions is given by:

$$\mathcal{L}^{(0)} = \mathcal{L}_s^{(0)} + \mathcal{L}_w^{(0)} , \quad (2.2)$$

with the strong interaction Lagrangian:

$$\mathcal{L}_s^{(0)} = \frac{F_0^2}{4} (\langle u_\mu u^\mu \rangle + \langle \chi_+ \rangle) , \quad (2.3)$$

and the $\Delta S = 1$ Lagrangian $\mathcal{L}_w^{(0)}$:

$$\mathcal{L}_w^{(0)} := C F_0^4 g_8 \langle \Delta u_\mu u^\mu \rangle ; \quad \Delta := u \lambda_6 u^\dagger , \quad (2.4)$$

where I introduce only the operator which dominates the contribution to the $I = 0$ part of the amplitude. $\mathcal{L}_w^{(0)}$ transforms like $(8, 1)$ under $SU(3)_L \otimes SU(3)_R$.

In addition to the lowest order Lagrangians $\mathcal{L}_s^{(0)}$ and $\mathcal{L}_w^{(0)}$, I will also use the NLO Lagrangian $\mathcal{L}_w^{(1)}$ [11, 12]:

$$\mathcal{L}_w^{(1)} = C F_0^2 g_8 \sum_{i=1}^{37} N_i^{(1)} W_i^{(1)} , \quad (2.5)$$

and the NNLO Lagrangian:

$$\mathcal{L}_w^{(2)} = C g_8 \sum_{i=1}^N N_i^{(2)} W_i^{(2)} , \quad (2.6)$$

with the respective coefficients:

$$N_i^{(1)} = (\mu c)^{-\varepsilon} \left(N_i^{(1)r}(\mu, \varepsilon) + Z_i^1 \Lambda \right) , \quad (2.7)$$

$$N_i^{(2)} = (\mu c)^{-2\varepsilon} \left(N_i^{(2)r}(\mu, \varepsilon) + Z_i^{22} \Lambda^2 + (Z_i^{21} + Z_{iL}^{21}(\mu, \varepsilon)) \Lambda \right) , \quad (2.8)$$

where $Z_{iL}(\mu)$ is a coefficient originating from a vertex of $\mathcal{L}^{(1)}$. The notation is:

$$\Lambda = \frac{1}{(4\pi)^2} \frac{1}{\varepsilon} ; \quad \varepsilon = \frac{1}{4-d} . \quad (2.9)$$

3 Chiral extrapolation

For a lattice calculation of the $K \rightarrow \pi\pi$ amplitude, one normally uses a tree level PCAC relation to relate the former to the $K^0 \rightarrow \pi^0$ and $K^0 \rightarrow |0\rangle$ amplitude [2]. The starting point is the lowest order Lagrangian, Eq. 2.4, which implies the relation²:

$$\mathcal{A} = \mathcal{A}_{\text{red.}} + \mathcal{O}(\hbar) , \quad (3.1)$$

with:

$$\begin{aligned} \mathcal{A} &:= \langle \pi^0 \pi^0 | \mathcal{H}_w^{(8,1)} | K^0 \rangle , \\ \mathcal{A}_{\text{red.}} &:= -i \frac{1}{F} \frac{\Delta_{\text{ph.}}}{m^2} \underbrace{\langle \pi^0 | \mathcal{H}_w^{(8,1)} | K^0 \rangle}_{=: \mathcal{A}_{\text{red.}}^1} + \frac{1}{2} \frac{1}{F^2} \frac{\Delta_{\text{ph.}}}{\Delta} \underbrace{\langle 0 | \mathcal{H}_w^{(8,1)} | K^0 \rangle}_{=: \mathcal{A}_{\text{red.}}^2} . \end{aligned} \quad (3.2)$$

I use the notation:

$$\Delta := m_K^2 - m_\pi^2 ; \quad m^2 := p_K p_\pi , \quad (3.3)$$

for the meson mass difference and intermediate meson masses which are evaluated on the lattice. $\Delta_{\text{ph.}}$ corresponds to the physical value of Δ .

Since this relation is derived from the tree level Lagrangian, it does not take into account any loop contributions, in particular no re-scattering effects between the two pions (final state interactions). However, these physical phenomena are reproduced in a lattice simulation, and consequently one has to find a way to split a lattice result into a part corresponding to the tree level and the higher order contributions.

To do so, we write Eq. (3.1) again, noting that it is an exact identity if one identifies all the matrix elements with the corresponding lowest order quantities ($X = \sum_{n=0}^{\infty} \hbar^n X^{(n)}$):

$$\mathcal{A}^{(0)} = \mathcal{A}_{\text{red.}}^{(0)} , \quad (3.4)$$

and re-introduces the higher order corrections with appropriate quotients:

$$\mathcal{A} := q \mathcal{A}^{(0)} ; \quad \mathcal{A}_{\text{red.}}^1 = q_1 \mathcal{A}_{\text{red.}}^{1(0)} ; \quad \mathcal{A}_{\text{red.}}^2 = q_2 \mathcal{A}_{\text{red.}}^{2(0)} . \quad (3.5)$$

²The Δ 's here shouldn't be confused with the chiral operator used in Eq. (2.4).

With these definition one can write ($\langle A_\mu^X \rangle = \langle 0 | A_\mu | X \rangle = \mathbf{1} F p_\mu^X$; $F = q_F F_0$ ³):

$$\mathcal{A} = q \Delta_{\text{ph.}} \left(-\mathbf{1} F_0 \frac{q_F^2}{q_1} \frac{\mathcal{A}_{\text{red.}}^1}{\langle A_\mu^\pi \rangle \langle A_\mu^K \rangle} + \frac{1}{2} \frac{q_F^2}{q_2} \frac{\mathcal{A}_{\text{red.}}^2}{(\langle A_\mu^K \rangle^2 - \langle A_\mu^\pi \rangle^2)} \right) . \quad (3.6)$$

The expression in brackets on the RHS of Eq. (3.6) corresponds to the LEC g_8 and is thus independent of quark masses. Consequently one is free to take the chiral limit $m_q \rightarrow 0$ of this quantity, which takes q_1 , q_2 and q_F to their chiral values of 1:

$$\mathcal{A} = q \Delta_{\text{ph.}} \left(-\mathbf{1} F_0 \lim_{m_q \rightarrow 0} \frac{\mathcal{A}_{\text{red.}}^1}{\langle A_\mu^\pi \rangle \langle A_\mu^K \rangle} + \frac{1}{2} \lim_{m_q \rightarrow 0} \frac{\mathcal{A}_{\text{red.}}^2}{(\langle A_\mu^K \rangle^2 - \langle A_\mu^\pi \rangle^2)} \right) . \quad (3.7)$$

One evaluates the RHS of Eq. (3.6) for various quark masses on the lattice and performs the extrapolation to the chiral limit, i.e. Eq. (3.7). Examples of how this procedure works in practice can be found in [13, 14].

The rest of this paper will be concerned about q :

$$q = \frac{\mathcal{A}}{\mathcal{A}^{(0)}} = 1 + \sum_{n=1}^{\infty} \hbar^n \delta q^{(n)} , \quad (3.8)$$

which is needed on the RHS of Eq. (3.7) in order to bring the chiral limit value of the $K^0 \rightarrow \pi\pi$ amplitude (i.e. $\Delta_{\text{ph.}}$ times the expression in brackets) back to the real world with the physical (nonzero) quark masses.

In section 4 I discuss the NLO corrections to q , emphasizing the contribution of the chiral logs. Subsequently, in section 5, I will include the double logs, which are a part of $\delta q^{(2)}$, into the discussion. The calculation of these is outlined in appendix B.

4 The chiral logs of $K^0 \rightarrow \pi\pi$ at NLO

Let me start by providing the NLO logarithmic corrections to the $K^0 \rightarrow \pi\pi$ amplitude to the lowest chiral order result. These corrections were first calculated by Bijnens [15].

The $K^0 \rightarrow \pi\pi$ amplitude is expanded in its \hbar order:

$$\mathcal{A} = \sum_{n=0}^{\infty} \hbar^n \mathcal{A}^{(n)} . \quad (4.1)$$

At leading order, we have:

$$\mathcal{A}^{(0)} = -\sqrt{2} \mathbf{1} C F_0 g_8 (m_K^2 - m_\pi^2) . \quad (4.2)$$

Altogether six diagrams (see Fig. 5) contribute to the full NLO result, which is provided in Eq. (C.1). The ν -dependence of $\mathcal{A}^{(1)}$ is drawn as a full line in Fig. 1.

³I do not differentiate between F_π and F_K since they will only be relevant in their chiral limit where they coincide.

Restricting the NLO contributions to the chiral logs using the approximations as outlined in appendix A, one gets the expression:

$$\mathcal{A}_{\log}^{(1)} = -\sqrt{2}iCF_0g_8m_K^2 \left(1 - m_K^2(L_\pi(\nu) + \frac{1}{4}L_K(\nu)) + \frac{27}{8}m_\pi^2L_\pi(\nu) + \dots \right) , \quad (4.3)$$

where I used the notation (ν : renormalization scale):

$$L_X(\nu) := \frac{1}{(4\pi F)^2} \ln\left(\frac{m_X^2}{\nu^2}\right) ; \quad X = \pi, K, \eta . \quad (4.4)$$

The approximation corresponding to Eq. (4.3) is drawn as a dashed gray line in Fig. 1, closest to the full result. The nearby lightly dashed line corresponds to the leading order result plus the full logarithmic NLO contribution.

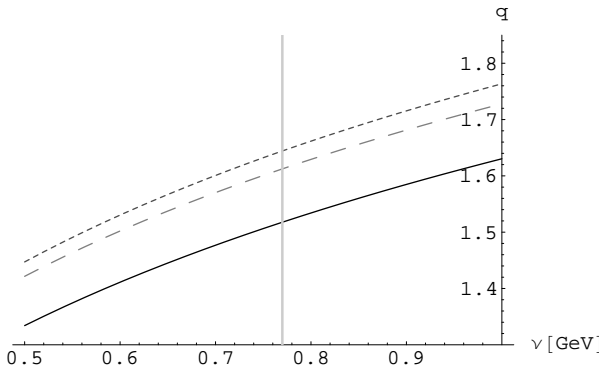


Figure 1: The renormalization scale dependence of $q = |\mathcal{A}^{(1)}|/\mathcal{A}^{(0)}$ in terms of F_0 . The full line corresponds to the full expression, Eq. (C.1), with all LEC's $N_i^{(1)r}(\nu)$ set to zero. The lightly dashed gray line is the approximation taking at NLO only the (full) chiral logs into account. The dashed gray line below, closest to the full result, corresponds to the approximation given in Eq. (4.3).

In order to get an estimate for $q^{(1)} = |\mathcal{A}^{(1)}|/\mathcal{A}^{(0)}$, I will use the natural scale of CHPT, $4\pi F_\pi/\sqrt{N_f} \simeq m_\rho$, N_f being the number of dynamical fermions [16], where one expects the values of the LEC's not to have acquired too large values due to running. Using F_0 as input, one gets:

$$q^{(1)}(\nu = 0.77\text{GeV}) \simeq 1.52 \text{ (1.61)} , \quad (4.5)$$

which corresponds to the full amplitude, as given in appendix C, with all NLO LEC's set to zero; The number in brackets is the value of the approximation given in Eq. (4.3). Please note (Fig. 1) that the latter simple expression is able to mimic the full amplitude (with $N_i^{(1)r}(\nu) \equiv 0$) with an accuracy well below 10%. Since the lack of knowledge of the LEC's introduces an error of the same order or probably even higher, it does not really make a big difference if one uses the simple form of Eq. (4.3) instead of the full expression, Eq. (C.1).

5 Chiral extrapolation including the double logs

In this section I include the double log contributions to \mathcal{A} into the discussion of the factor q . The more technical details of how to calculate these is outlined in appendix B. Using this the approximation, we have:

$$\begin{aligned}\mathcal{A} &\cong \mathcal{A}^{(0)} + \delta\mathcal{A}^{(1)} + \delta\mathcal{A}_{\log}^{(2)} , \\ &= \mathcal{A}^{(0)} \left(1 + \delta^{(1)} + \delta_{\log}^{(2)} \right) .\end{aligned}\quad (5.1)$$

I will again work with the approximations for the chiral logs as outlined in appendix A, i.e. Eq. (A.2) and (A.3).

In this scheme, the following terms contribute to the amplitude:

$$\tilde{\delta}_{\log}^{(2)}(\nu) = m_K^4 \left(\tilde{\alpha}_{\pi K}^{(2)} L_{\pi}(\nu) L_K(\nu) + \tilde{\alpha}_{KK}^{(2)} L_K(\nu)^2 + \tilde{\alpha}_{MM}^{(2)} L_M(\nu)^2 \right) , \quad (5.2)$$

where I introduce an intermediate meson m_M for the double log terms which were calculated via the leading two-loop divergences. For these one cannot determine whether pions or kaons in the loops generate the logs. The first two terms in Eq. (5.2) originate from diagrams where we performed the loop integration explicitly (Terms proportional to L_{π}^2 are not generated). In the following I will parametrize the intermediate mass M by:

$$m_M(t) = m_{\pi}^t m_K^{1-t} \quad t \in [0, 1] .$$

Similarly as for the NLO result, Eq. (5.2) is not well defined in the limit where $m_{\pi} \rightarrow 0$ or $m_M \rightarrow 0$. One should again view Eq. (5.2) only to be an allowed approximation for the double logs for the physical (nonzero) masses.

The term $m_K^4 \tilde{\alpha}_{\pi K}^{(2)} L_{\pi}(\nu) L_K(\nu)$ in Eq. (5.2) has a similar origin like the analogue piece of the NLO result, while the third term, $m_K^4 \tilde{\alpha}_{MM}^{(2)} L_M(\nu)^2$, is generated by graphs with 1PI two-loop subdiagrams. We will see below that the double log contribution is rather sensitive on the value chosen for m_M . The 1PI two-loop diagrams contributing to this term are either of the "eight" or "sunrise" topology. For the former, the loop integrals are factorized, leading only to chiral logs of the form $m_X^2 L_X$, from which follows that $m_M = m_K$ or $t = 0$ for this class of diagrams. For the sunrise topology, however, terms of the form $m_K^4 L_{\pi}^2$ and $m_K^4 L_{\pi} L_K$ can be generated [17, 4], presumably shifting t to a nonzero value. I am not aware of a method how to accurately estimate the value of t . However, it was already noted by Bijnens et al. in [6], discussing the double logs in the strong sector, that a large value of t leads to unrealistic large double log contributions (They used $t = 1/2$). In the following I will use the conservative values $t \in [0, 0.1]$. The inability to estimate t in an exact way unfortunately hinders us in making very accurate predictions for q .

The double logs originate from four classes of diagrams, as outlined in appendix B. The separate contributions of these diagrams as well as more technical details can be found there. Here I provide only the final result:

$$\begin{aligned}\mathcal{A}_{\log}^{(2)}(\nu) &= -\sqrt{2}i C F_0 g_8 m_K^2 \left(1 - m_K^2 (L_{\pi}(\nu) + \frac{1}{4} L_K(\nu)) + \frac{27}{8} m_{\pi}^2 L_{\pi}(\nu) \right. \\ &\quad \left. + m_K^4 \left(-\frac{221}{108} L_{\pi}(\nu) L_K(\nu) - \frac{1349}{12960} L_K(\nu)^2 + \frac{7703}{648} L_M(\nu)^2 \right) + \dots \right) ,\end{aligned}\quad (5.3)$$

for the amplitude given in terms of F_0 ⁴.

Fig. 2 shows the ν dependence of q using the full NLO amplitude ($N_i^r(\nu) \equiv 0$) plus the double log contribution. Fig. 3 illustrates the accuracy of the approximation, Eq. (5.3), based on the use of Eq. (A.2) and (A.3), by comparing it with q calculated with the "full" result for the double logs. Fig. 4 displays the dependence of q_2 on the intermediate mass m_M parametrized by t .

As already noted in [15], the ν -dependence of q is quite strong. This dependence would be canceled by the LEC's, whose values are unknown and consequently set to zero at all values of ν , making exact predictions impossible. Employing the same reasoning as in section 4, I will use the renormalization scale $\nu = 0.77\text{GeV}$ in order to get an estimate of q . Various values of q at $\nu = 0.77\text{GeV}$ at different values of t are provided in Table 2.

	$q(\nu = 0.77\text{GeV})$
NLO	1.52 (1.61)
NLO + Double Logs ($t = 0.00$)	1.64 (1.75)
NLO + Double Logs ($t = 0.05$)	1.77 (1.88)
NLO + Double Logs ($t = 0.10$)	1.91 (2.03)

Table 2: The "enhancement factor" q at NLO with and without the inclusion of the double logs at $\nu = 0.77\text{GeV}$, using F_0 as input. The numbers correspond to the full NLO expression provided in appendix C with $N_i^r(\nu) \equiv 0$. The numbers in brackets correspond to the approximation as given in Eq. (5.3).

6 Impact on present lattice results

In this section I discuss the implication of the presented results on the values for the $\text{Re}(A_0)$ provided from lattice simulations.

The experimental value of $\text{Re}(A_0)$ is:

$$\text{Re}(A_0)^{\text{exp.}} = 33.3 \cdot 10^{-8}\text{GeV} \quad (6.4)$$

The CP-PACS collaboration calculated $\text{Re}(A_0)$ using quenched domain wall fermions [13]. In their paper they use the reduced matrix element, Eq. (3.2), and extrapolate it to the chiral limit, analogously to Eq. (3.6). For this means they either use a quadratic polynomial (Fit I: $\text{Re}(A_0) = \xi_0 + \xi_1 m_M^2 + \xi_2 (m_M^2)^2$) or chiral logarithms (Fit II: $\text{Re}(A_0) = \xi_0 + \xi_1 m_M^2 + \xi_2 m_M^2 L_M$). The outcome is:

$$\text{Re}(A_0)_{\text{chiral limit}}^{\text{CP-PACS}} = \begin{cases} 16.5 \cdot 10^{-8}\text{GeV} & \text{Fit I} \\ 20.7 \cdot 10^{-8}\text{GeV} & \text{Fit II} \end{cases}$$

⁴ F_0 should also be used in the definition of the L_X , Eq. (4.4).

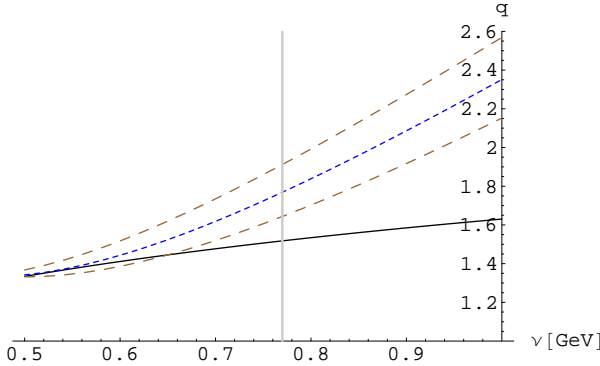


Figure 2: The renormalization scale dependence of q at NLO (full line) and at NLO with the double log contributions included with an intermediate mass $m_M(t = 0)$ (lowest dashed line), $m_M(t = 0.05)$ (intermediate lightly dashed line) and $m_M(t = 0.10)$ (uppermost dashed line) respectively. All $N_i^r(\nu)$'s are set to zero. The most natural choice to get an estimate of q is to set all LEC's to zero at the natural scale of CHPT, $\nu \simeq m_\rho$, which results in the values 1.52 (NLO), 1.64 ($t = 0$), 1.77 ($t = 0.05$) and 1.91 ($t = 0.1$) respectively.

They do, however, not implement higher order CHPT corrections to the $K \rightarrow \pi\pi$ amplitude, i.e. they use $q = 1$. If we take $q = 1.77$, corresponding to $\nu = 0.77\text{GeV}$ and $t = 0.05$ (see section 5), one gets the values:

$$\text{Re}(A_0)^{\text{CP-PACS}} = \begin{cases} 29.2 \cdot 10^{-8}\text{GeV} & \text{Fit I} \\ 36.6 \cdot 10^{-8}\text{GeV} & \text{Fit II} \end{cases}$$

Since the above numbers can only serve as an order of magnitude estimate, I do not provide any error bars for them. The errors for q are probably in the range of 20% or even higher. The important statement one can however extract from the above numbers is that the corrections due to q can explain the discrepancy between the experimental number and the lattice value (which corresponds to the chiral limit value of $\text{Re}(A_0)$).

The RBC collaboration [14] which also used quenched domain wall fermions in their simulations account for the chiral logs of the $K \rightarrow \pi\pi$ amplitude, but use the old result of Bijnens [15], which did not take into account all the diagrams contributing to these and is therefore incorrect (see section A). Their result with and without the "old" chiral logs is:

$$\text{Re}(A_0)^{\text{RBC}} = \begin{cases} 20.9 \cdot 10^{-8}\text{GeV} & \text{chiral limit} \\ 29.6 \cdot 10^{-8}\text{GeV} & \text{with "old" chiral logs} \end{cases}$$

If we again implement the factor $q = 1.77$, we get:

$$\text{Re}(A_0)^{\text{RBC}} = 37.0\text{GeV} , \quad (6.5)$$

which agrees well with the experimental value within the rather large errors one has to assume.

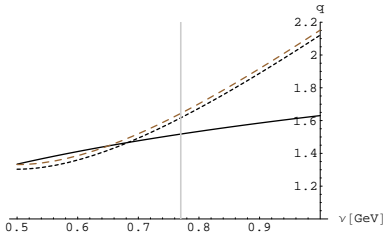


Figure 3: The ν dependence of q for $m_M(t = 0) = m_K$ using the full result of the double log contribution (lightly dashed line) and the approximation given in Eq. (5.3) (upper dashed line). The full line correspond to the NLO result.

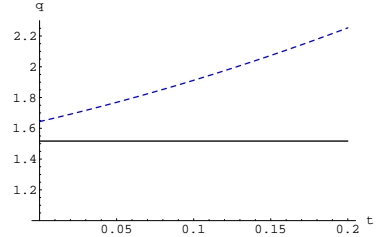


Figure 4: The dependence on q at $\nu = 0.77\text{GeV}$ on the meson mass value used in the logarithm L_M in Eq. (5.3), parametrized by $m_M = m_\pi^t m_K^{1-t}$. The full line corresponds to the NLO value.

7 Conclusion

I have calculated the contributions of the (leading) chiral logs at NLO and at NNLO using Renormalization Group methods. I studied the result numerically and confirm and even reinforce the known result that these contributions are quite large [15]. With the approximations and assumptions used in this paper, the lowest order $K \rightarrow \pi\pi$ amplitude is enhanced by a factor between 1.64 and 1.91 due to loop effects, depending rather strongly on the average value employed for the mass of the mesons in the loops generating the logs, but in all cases further enhancing the NLO value of 1.52. The numerical results provided here thus point in the right direction to explain the $\Delta I = 1/2$ rule as a low energy QCD effect.

The above given numbers can only serve as a rough estimate of the higher order contributions, since we are not in a position to include the contributions of the LEC's at NLO, and other additional contributions at NNLO. However, given that it is not possible to calculate the higher order LEC's in this sector so far, these estimates are yet the best one can do with an acceptable effort to get an idea of the correction to the lowest order result one has to expect.

Even though not providing accurate numbers, the calculation presented here shows that one has to anticipate rather large higher order CHPT corrections to the lowest order result of the $K \rightarrow (\pi\pi)_{I=0}$ amplitude. This again indicates the importance to make further efforts to include these contributions, physically corresponding to the effects caused by the interaction between the three mesons, in an accurate way.

Acknowledgment

I would like to thank Gilberto Colangelo for participation in the early stages of this work and many very helpful discussions.

This work was supported by the Swiss National Science Foundation.

A Detailed discussion of the NLO contributions

In this section I give a detailed discussion of the NLO corrections and the approximations I made. The diagrams which contribute are drawn in Fig. 5.

Below I will work with the approximation where one restricts the NLO corrections to the

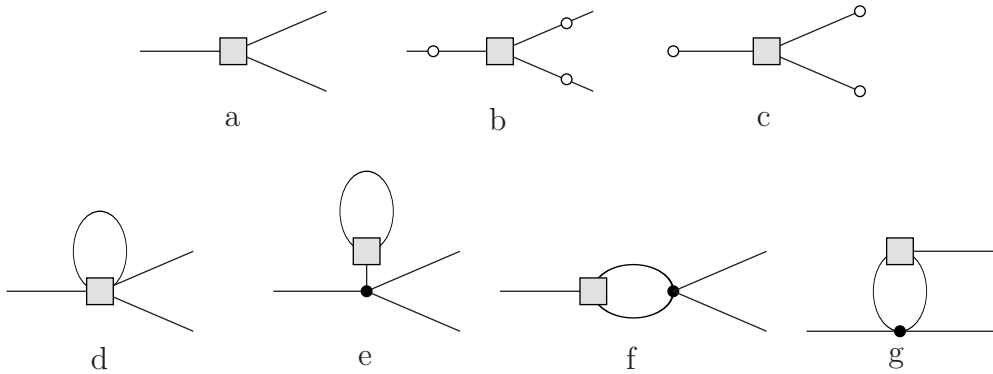


Figure 5: Diagrams contributing to the $K^0 \rightarrow \pi\pi$ amplitude at NLO: a: Leading order, b: Wave-function renormalization, c: Decay constant renormalization, d: first tadpole, e: second tadpole, f: first unitary correction, g: second unitary correction. Not drawn are the two counter-term diagrams.

chiral logs:

$$\begin{aligned} \mathcal{A} &= \mathcal{A}^{(0)}(1 + \delta\mathcal{A}_{\log}^{(1)} + \dots) , \\ &= \mathcal{A}^{(0)}(1 + \alpha_\pi L_\pi(\nu) + \alpha_K L_K(\nu) + \alpha_\eta L_\eta(\nu) + \dots) . \end{aligned} \quad (\text{A.1})$$

The α_X above are polynomials quadratic in the meson masses.

In addition I neglect all m_π^2 contributions relative to m_K^2 in the polynomials (α 's) and write the resulting quantities with a tilde:

$$\alpha_X = m_K^2 \tilde{\alpha}_X + \mathcal{O}(m_\pi^2) . \quad (\text{A.2})$$

This approximation will be particularly useful in the case of the NNLO contributions. Furthermore I identify the logarithms:

$$L_K(\nu) \simeq L_\eta(\nu) . \quad (\text{A.3})$$

All following quantities for which the above approximations, Eqs. (A.2) and (A.3), are employed will be written with a tilde.

Using these, I get for $\delta\tilde{\mathcal{A}}_{\log}^{(1)}$:

$$\delta\tilde{\mathcal{A}}_{\log}^{(1)}(\nu) = m_K^2 \left(-L_\pi(\nu) - \frac{1}{4}L_K(\nu) \right) . \quad (\text{A.4})$$

This result corresponds to the lowest order amplitude in Eq. (4.2), expressed in terms of the bare decay constant ⁵. In the following I will write all quantities in terms of F_0 ; Expressing amplitudes in terms of the renormalized decay constant F_π increases generally the ν dependence artificially. I use the values:

$$F_\pi = 0.0924 \text{ GeV} ; \quad \frac{F_\pi}{F_0} = 1.06 , \quad (\text{A.5})$$

which should be precise up to two loop order [18]. Using this approach, the results will not get distorted by omitting known contributions to F_π like LEC's etc. .

Please note that Eq. (A.4) does not have a well defined limit $m_\pi \rightarrow 0$. The above approximation is meant to be used with the physical values of the meson masses. If we leave this regime and take the $m_\pi \rightarrow 0$ limit, one has to include the associated \bar{J} function in order to cancel the occurring divergence. In principle it would be aesthetically more appealing to have an expression at hand that respects the underlying chiral symmetries and limits, which could be accomplished by re-introducing parts of \bar{J} contributions in Eq. (A.4). I will however limit ourselves to the strict use of the chiral logs as unambiguously defined in Eq. (1.1), since this approach defines a well-defined setting.

The separate contributions of the diagrams to $\tilde{\alpha}_\pi$, $\tilde{\alpha}_K$ and $\tilde{\alpha}_\eta$ are given in Table 3.

In order to obtain an expression which agrees with the full logarithmic corrections at the

Diagram	a	b	c	d	e	f	g	total
$\tilde{\alpha}_\pi$	0	0	0	0	0	-1	0	-1
$\tilde{\alpha}_K$	0	7/12	1/2	-2	1/3	-1/6	1/2	-1/4
$\tilde{\alpha}_\eta$	0	1/6	0	-22/27	8/27	0	23/27	1/2
Sum	0	3/4	1/2	-76/27	17/27	-7/6	73/54	-3/4

Table 3: The various contributions of the logs of the separate diagrams.

5 – 10% level, I also include the most dominant subleading contribution ⁶:

$$\mathcal{A}_{\log}^{(1)} = -\sqrt{2}iCF_0g_8m_K^2 \left(1 - m_K^2 \left(L_\pi(\nu) + \frac{1}{4}L_K(\nu) \right) + \frac{27}{8}m_\pi^2L_\pi(\nu) + \dots \right) . \quad (\text{A.6})$$

In the first paper treating these corrections the following value was provided [15]:

$$\tilde{\mathcal{A}}_{\log}^B(\nu) \sim \frac{m_K^2}{F^3} \left(1 - \frac{97}{27}m_K^2L_K(\nu) \right) . \quad (\text{A.7})$$

⁵Replacing F_0 with F_π shifts the constants in front of the chiral logs.

⁶This is necessary since the coefficient of the subleading term is a factor 3 times larger than the sum of the leading coefficients.

Writing the result, Eq. (A.4), with the above normalization, using $L_\pi \simeq L_K \simeq L_M$, in terms of F_0 and F_π respectively, one gets:

$$\tilde{\mathcal{A}}_{\log} \sim \frac{m_K^2}{F_0^3} \left(1 - \frac{5}{4} m_K^2 L_M(\nu) \right) , \quad (\text{A.8})$$

$$\sim \frac{m_K^2}{F_\pi^3} \left(1 - \frac{11}{4} m_K^2 L_M(\nu) \right) . \quad (\text{A.9})$$

Equating L_π and L_K I found numerically to be a rather crude approximation; I have checked that this identification results in values which disagree by approximately a factor of two from the full result of the logarithms.

In the original paper [15] the diagram e in Fig. 5 is missing. This together with a different treatment of the $m_K^2 L_\pi$ contributions generated by diagram f is the origin of the above discrepancy⁷. Let us point out in this context that I checked my full NLO $K \rightarrow \pi\pi$ amplitude on which the results above are based with the output of the Mathematica package provided in [19] and found complete agreement.

B The calculation of the $K \rightarrow \pi\pi$ double logs

In this section I provide the details of the calculation of the double logs of the $K \rightarrow \pi\pi$ amplitude:

$$\mathcal{A} = \langle \pi(p_1) \pi(p_2) (I = 0) | \mathcal{H}_w^{(8,1)}(q_w) | K(q_K) \rangle . \quad (\text{B.10})$$

Throughout the calculation, I allowed the weak Hamiltonian to carry the momentum q_w , a setting which can be used to account for the final state interactions dispersively [20]. However, since the resulting expressions get too cumbersome, I will only provide the results for the physical case, $q_w = 0$ ⁸. As in the previous sections I will exclusively consider the octet part of the nonleptonic weak chiral Lagrangian.

The double logs of \hbar -order 2 contributing to Eq. (B.10) are produced by two-loop diagrams, each loop contributing one logarithm. The amplitude can be expanded in the \hbar -order :

$$\mathcal{A} = \mathcal{A}^{(0)} + \mathcal{A}^{(1)} + \mathcal{A}^{(2)} + \mathcal{O}(\hbar^3) . \quad (\text{B.11})$$

All "genuine" double logs originating from graphs with a two-loop 1PI subgraph can be calculated with the $\frac{1}{\varepsilon^2}$ poles in the two-loop counterterm, depicted in Fig.6, diagrams a and b. Additionally, there are graphs with two independent one loop subgraphs, corresponding to diagram c. A further contribution originates from LSZ/wavefunction renormalizations of graphs of lower chiral order, $\mathcal{O}(p^2, p^4)$. Finally, the lowest order masses and decay constants of these lower order graphs have to be shifted to their renormalized physical value, up to the required chiral order. This two last contributions are represented by diagram d.

⁷private communication with the author of [15].

⁸The full expression can be obtained from the author.

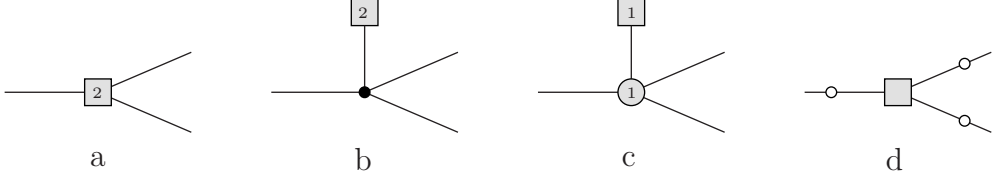


Figure 6: Diagrams contributing to the $K^0 \rightarrow \pi\pi$ amplitude at NNLO. The square boxes represent 1PI loop graphs with one insertion of a weak vertex and loop order given inside the boxes. The circles are the analogues with no weak vertices. a: genuine 1PI, b: genuine 1PI subgraph attached to a strong tree vertex, c: A weak and a strong subgraph with loop order 1 respectively, d: Lower order graphs (represented by a box with no associated loop order) which experience mass/decay constant shifts or LSZ renormalization. I have not drawn the associated counterterm diagrams. However, for diagram a and b I calculated the double logs via their associated counterterms, and for diagram c and d I used partially the same approach.

For the graphs which consist of two one-loop subgraphs, diagram c, one can calculate the subgraphs separately (One-loop $K\pi$ scattering and $K \rightarrow |0\rangle$). However, there is a subtlety one has to account for: Since the Kaon which propagates on the one-particle-reducible line of these graphs is offshell, one cannot cut the graphs and identify the two resulting subgraphs as physical processes, since for this to be true, the Kaon would have to be onshell (an asymptotic state). As a consequence, one cannot treat the "genuine" graphs a and b, the 1PR graph c, and the LSZ/wavefunction contributions, diagram d, separately. In particular, only the sum of these graphs will cancel all divergences.

For the graph c, I calculate the double logs explicitly by multiplying the two separate one-loop graph expressions, and get a residual $\frac{1}{\varepsilon^2}$ divergence. This divergence, however, can be absorbed into the counterterm of the remaining, $\frac{1}{\varepsilon^2}$ generating graphs. If we proceed in this way, the shifted counterterm will cancel the $\frac{1}{\varepsilon^2}$ divergences of the rest of the diagrams. For those one can calculate the double logs as follows: All loop divergences have the structure (see Eq. (1.1)):

$$\mathcal{Q} = \nu^{-\varepsilon} \left(\Lambda - \mu_M(\nu) + \dots \right) , \quad (\text{B.12})$$

which ensures scale independence. I used the definition:

$$\mu_X(\nu) = \frac{1}{2} \frac{m_X^2}{F^2} L_X(\nu) .$$

If we define a basis $W_i^{(2)}$ of operators for the \hbar -order 2 Lagrangian, the sum of the divergences of all "genuine" two-loop diagrams will result in the structure:

$$Cg_8 \sum_{i=1}^N \alpha_i W_i^{(2)} \mathcal{Q}^2 = Cg_8 \nu^{-2\varepsilon} \sum_{i=1}^N \alpha_i W_i^{(2)} \left(\Lambda^2 - 2\Lambda \mu_M(\nu) + \mu_M(\nu)^2 + \dots \right) . \quad (\text{B.13})$$

Note that one has generated a nonlocal divergence ΛL_M . These structures will, however, be canceled by the contribution of one loop diagrams with one insertion of a vertex from $\mathcal{L}^{(1)}$. Thus, the sum of the divergences of all diagrams will be free of nonlocalities and be canceled by the Lagrangian $\mathcal{L}_w^{(2)}$, Eq. (2.6).

Since the double logs of the loops always show up in the combination $\Lambda^2 + \mu_M^2$, see Eq. (B.13), and the Λ^2 divergences have to be canceled by the $Z_i^{22}\Lambda^2$ term in Eq. (2.8), the double logarithms can be calculated as follows (The $\bar{\mathcal{L}}_i^{22}$'s correspond to the $1/\varepsilon^2$ poles of the sum of all loop contribution, $\bar{\mathcal{L}}_i^{22} = -Z_i^{22}$):

$$\begin{aligned} Cg_8\nu^{-2\varepsilon} \sum \bar{\mathcal{L}}_i^{22} W_i^{(2)} \mu_M(\nu)^2 &= -Cg_8\nu^{-2\varepsilon} \sum Z_i^{22} W_i^{(2)} \mu_M(\nu)^2 , \\ &= -Cg_8\nu^{-2\varepsilon} \mathcal{A}_2^2 \mu_M(\nu)^2 . \end{aligned} \quad (B.14)$$

Note that of the chiral order p^2 and p^4 graphs, which are affected by wavefunction and LSZ renormalization, only the tree graph will generate $\frac{1}{\varepsilon^2}$ terms: the one-loop graph is finite and the wavefunction and LSZ renormalization shifts on the one-loop graphs are of \hbar -order 1 and can therefore only introduce $\frac{1}{\varepsilon}$ divergences, and consequently we can discard the one-loop graph from the list of terms which contribute to $\frac{1}{\varepsilon^2}$ divergences.

The final result of this calculation, split into a sum of contributions originating from the different diagrams drawn in Fig. 6, is provided in Table 4.

Diagram	$\tilde{\alpha}_{\pi K}^{(2)}$	$\tilde{\alpha}_{KK}^{(2)}$	$\tilde{\alpha}_{MM}^{(2)}$
a	0	0	18599/1944
b	0	0	-1213/972
c	-17/27	269/540	4/3
d	- 17/12	-1561/2592	181/81
Sum	- 221/108	- 1349/12960	7703/648

Table 4: The various contributions of the double logs of the separate diagrams, which are drawn in Fig 6.

C One loop amplitudes

For completeness I provide here the full one loop $K^0 \rightarrow \pi\pi$ amplitude as well as the $K^0\bar{K}^0 \rightarrow \pi\pi$ and $K^0 \rightarrow |0\rangle$ amplitudes, needed in intermediate steps of the double log computation. All these amplitudes have been calculated with the generalized kinematics, where the weak Hamiltonian is allowed to carry momentum. The results displayed below correspond however to the amplitudes with the weak Hamiltonian at rest. The general result can be obtained from the authors.

The functions used in the amplitudes given below are defined in appendix E.

The renormalization scale dependence of the LEC's $L_i^r(\nu), N_i^r(\nu)$, which cancels the ν -dependence of the chiral logarithms $\mu_X(\nu)$ will be suppressed in the following. All calculations have been performed with FORM [21].

C.1 $K^0 \rightarrow \pi\pi$

$$\begin{aligned} \langle \pi^0 \pi^0 | \mathcal{H}_w^{(8,1)} | K^0 \rangle = & \\ & \frac{i C F_\pi g_8 \Delta}{\sqrt{2}} \left(-2 + \frac{\hat{N}}{F^2} \left(-\frac{8}{9} m_\pi^2 + 2 m_K^2 \right) + \left(-\frac{27}{2} + 4 \frac{m_K^2}{m_\pi^2} \right) \mu_\pi + \mu_K + \left(\frac{37}{18} \frac{m_\pi^2}{m_\eta^2} - 2 \frac{m_K^2}{m_\eta^2} \right) \mu_\eta \right. \\ & - \frac{1}{2} \frac{m_\pi^4}{\Delta} (L_\pi - L_\eta) + 4 \frac{m_\pi^2}{F_\pi^2} (8 L_4^r + 6 L_5^r - 2 N_5^r - 4 N_7^r - N_8^r + 2 N_{10}^r + 4 N_{11}^r + 2 N_{12}^r) \\ & + \frac{4 m_K^2}{F_\pi^2} (16 L_4^r + 2 L_5^r - N_5^r + 2 N_7^r - 2 N_8^r - N_9^r) - \frac{2 m_K^2 - m_\pi^2}{F_\pi^2} \bar{J}_{\pi\pi}(m_K^2) - \frac{1}{9} \frac{m_\pi^2}{F_\pi^2} \bar{J}_{\eta\eta}(m_K^2) \\ & \left. - \frac{1}{m_\pi^2 F_\pi^2} \left(\left(-\frac{1}{2} m_K^4 + 2 m_\pi^2 m_K^2 \right) \bar{J}_{\pi K}(m_\pi^2) + \frac{1}{6} m_K^4 \bar{J}_{K\eta}(m_\pi^2) \right) \right) + \mathcal{O}(\hbar^2) . \end{aligned} \quad (\text{C.1})$$

I checked the above result with the Mathematica program recently provided by [19].

C.2 $K^0 \bar{K}^0 \rightarrow \pi\pi$

$$\begin{aligned} \langle \pi\pi | \mathcal{H}_s | K^0(q_K) \bar{K}^0(q_{\bar{K}}) \rangle_{q_K^2 = m_K^2, q_{\bar{K}}^2 = 0} = & \\ & \frac{1}{2 F_\pi^2} \left(\frac{1}{3} m_K^2 + \Lambda \left(\frac{13}{90} m_\pi^2 - \frac{17}{45} m_K^2 \right) m_K^2 + \frac{\hat{N}}{F^2} \left(\frac{1}{9} m_\pi^2 m_K^2 - \frac{7}{12} m_K^4 \right) \right. \\ & + \mu_\pi \left(1 - \frac{m_K^2}{2 m_\pi^2} + \frac{m_K^2}{\Delta} \left(\frac{2}{3} - \frac{1}{6} \frac{m_K^2}{m_\pi^2} \right) \right) m_K^2 + \mu_K \left(\frac{11}{30} - \frac{1}{6} \frac{m_K^2}{m_\pi^2} + \frac{1}{6} \frac{m_K^4}{\Delta m_\pi^2} \right) m_K^2 \\ & \mu_\eta \left(\frac{1}{6} m_\pi^2 + \frac{1}{15} m_K^2 + \frac{m_\pi^2}{m_\eta^2} \left(\frac{1}{18} m_\pi^2 - \frac{1}{3} m_K^2 \right) \right) + L_4^r \left(-\frac{56}{3} m_\pi^2 m_K^2 + \frac{8}{3} m_K^4 \right) - \frac{20}{3} L_5^r m_\pi^2 m_K^2 \\ & + 32 L_6^r m_\pi^2 m_K^2 + L_8^r \left(\frac{8}{3} m_\pi^4 + 32 m_\pi^2 m_K^2 + \frac{8}{3} m_K^4 \right) + \bar{J}_\pi(m_K^2) \left(\frac{1}{6} m_\pi^2 - \frac{1}{3} m_K^2 \right) m_K^2 \\ & \left. + \frac{1}{4} \bar{J}_K(m_K^2) m_K^4 + \frac{1}{18} \bar{J}_\eta(m_K^2) m_\pi^2 m_K^2 + \bar{J}_{\pi K}(m_\pi^2) \left(-\frac{1}{3} + \frac{1}{12} \frac{m_K^2}{m_\pi^2} \right) m_K^4 \right) + \mathcal{O}(\hbar^2) . \end{aligned} \quad (\text{C.2})$$

C.3 $K^0 \rightarrow |0\rangle$

$$\begin{aligned} \langle 0 | \mathcal{H}_w^{(8,1)} | K^0(q_K) \rangle_{q_K^2 = 0} = & \\ & \frac{i C F_\pi^3 g_8}{\sqrt{2}} \left(-\frac{20}{3} \Delta m_K^2 \Lambda + 6 \mu_\pi m_\pi^2 - 4 \mu_K m_K^2 + \frac{2}{3} \mu_\eta (m_\pi^2 - 4 m_K^2) \right. \\ & \left. - 8 \Delta \left(+ 2 N_{10}^r m_K^2 + N_{11}^r (2 m_K^2 - m_\pi^2) + 8 N_{23}^r m_K^2 \right) \right) + \mathcal{O}(\hbar^2) . \end{aligned} \quad (\text{C.3})$$

Please note that the result given above correspond to the $K^0\bar{K}^0 \rightarrow \pi\pi$ and $K^0 \rightarrow |0\rangle$ amplitudes evaluated at the unphysical point where the momentum of one of the Kaons vanishes. I checked that I agree with the results of [22] for the $K^0\bar{K}^0 \rightarrow \pi\pi$ if I use the physical kinematics.

D Renormalized masses and wavefunction renormalization

In subsection D.1 I provide a list of the logarithmic contributions of the shifts of the bare masses to their renormalized value, up to NLO. In subsection D.2, the logarithmic contributions of the wavefunction renormalization shifts are given up to two-loop order.

D.1 Masses

For the masses I only need the $\hbar = 1$ corrections, since the tree Lagrangian given in Eq. 2.4 generates only dynamical masses:

$$m_X^2 = m_X^{(0)2}(1 + \delta m_X^2) ; \quad X = \pi, K, \eta . \quad (\text{D.1})$$

The log contributions of the NLO shifts thereof are [23]:

$$\begin{aligned} \delta m_{\pi \log}^{2(1)} &= (\mu_\pi - \frac{1}{3}\mu_\eta) , \\ \delta m_{K \log}^{2(1)} &= \frac{2}{3}\mu_\eta , \\ \delta m_{\eta \log}^{2(1)} &= -\frac{m_\pi^2}{m_\eta^2}\mu_\eta + (2 + \frac{2m_\pi^2}{3m_\eta^2})\mu_K + (\frac{7m_\pi^2}{9m_\eta^2} - \frac{16m_K^2}{9m_\eta^2}\mu_\eta)\mu_\eta . \end{aligned}$$

D.2 Wavefunction renormalization

$$Z_X = 1 + \delta Z_X ; \quad X = \pi, K, \eta ,$$

with:

$$\delta Z_X = \sum_{n=1}^{\infty} \hbar^n \delta Z_X^{(n)} .$$

We split $\delta Z_{X \log}^{(2)}$ into a piece linear (δ_1) and quadratic (δ_2) in the logarithms:

$$\delta Z_{X \log}^{(2)} = \delta_1 Z_{X \log}^{(2)} + \delta_2 Z_{X \log}^{(2)} .$$

The one-loop contribution is [23]:

$$\begin{aligned} \delta Z_{\pi \log}^{(1)} &= \frac{4}{3}\mu_\pi + \frac{2}{3}\mu_K , \\ \delta Z_{K \log}^{(1)} &= \frac{1}{2}\mu_\pi + \mu_K + \frac{1}{2}\mu_\eta , \\ \delta Z_{\eta \log}^{(1)} &= 2\mu_K . \end{aligned}$$

From $\delta Z_X^{(2)}$ one only needs $\delta_2 Z_{X \log}^{(2)}$ for the calculation. Since the wavefunction renormalization at this order is not available in the literature so far, I use the counterterm Lagrangian provided in [24] to obtain it. As already discussed in appendix B, one has to assume an unspecified intermediate meson mass m_M in the loops generating the chiral logs:

$$\begin{aligned}\delta_2 Z_{\pi \log}^{(2)} &= \left(\frac{113}{36} \frac{m_\pi^4}{m_M^4} - \frac{53}{18} \frac{m_\pi^2 m_K^2}{m_M^4} + \frac{73}{18} \frac{m_K^4}{m_M^4} \right) \mu_M^2 , \\ \delta_2 Z_{K \log}^{(2)} &= \left(\frac{17}{9} \frac{m_\pi^4}{m_M^4} - \frac{43}{36} \frac{m_\pi^2 m_K^2}{m_M^4} + \frac{32}{9} \frac{m_K^4}{m_M^4} \right) \mu_M^2 , \\ \delta_2 Z_{\eta \log}^{(2)} &= \left(\frac{5}{4} \frac{m_\pi^4}{m_M^4} - \frac{1}{6} \frac{m_\pi^2 m_K^2}{m_M^4} + \frac{19}{6} \frac{m_K^4}{m_M^4} \right) \mu_M^2 .\end{aligned}$$

The above expressions are not well-defined in the limit $m_M \rightarrow 0$, and one should only employ them for physical masses, i.e. $m_M > 0$ (See section 4).

E Loop integrals

All tadpole diagrams translate into the integral:

$$\begin{aligned}A_a &:= \int \frac{d^d l}{(2\pi)^d} \frac{1}{l^2 - m_a^2} , \\ &= \frac{1}{(4\pi)^{d/2}} \Gamma\left(1 - \frac{d}{2}\right) m_a^{\frac{d-2}{2}} , \\ &= (\nu c)^{-\varepsilon} m_a^2 \left(-2\Lambda + \frac{1}{(4\pi)^2} \ln\left(\frac{m_a^2}{\nu^2}\right) \right) + \mathcal{O}(\varepsilon) ,\end{aligned}\tag{E.1}$$

where I use:

$$\varepsilon := 4 - d \quad ; \quad \Lambda := \hat{N} \varepsilon ,\tag{E.2}$$

ν being the renormalization scale and c parameterizing the renormalization prescription ($c = -(\log(4\pi) - \gamma + 1)/2$ in \overline{MS}). The simplest integral which occurs in the diagrams corresponding to the unitarity corrections is:

$$J_{ab}(q^2) := -1 \int \frac{d^d l}{(2\pi)^d} \frac{1}{l^2 - m_a^2} \frac{1}{(l - q)^2 - m_b^2} .\tag{E.3}$$

Similar integrals to J with a polynomial in l in the numerator can be written in terms of a combination of A and J . J can be split into a divergent and finite part as follows:

$$J_{ab}(t) = -(2\Lambda + 2k_{ab}) + \bar{J}_{ab}(t) ,\tag{E.4}$$

with

$$k_{ab} = \frac{\hat{N}}{2} \frac{\log(m_a^2) - \log(m_b^2)}{m_a^2 - m_b^2}\tag{E.5}$$

and

$$\begin{aligned}
\bar{J}_{ab}(t) &= J_{ab}(t) - J_{ab}(0) , \\
&= \hat{N} \left(1 + \left(\frac{\Delta}{2t} - \frac{\Sigma}{2\Delta} \right) \log \left(\frac{m_a^2}{m_b^2} \right) - \frac{\tilde{\lambda}}{2t} \log \left(\frac{(t + \tilde{\lambda})^2 - \Delta^2}{(t - \tilde{\lambda})^2 - \Delta^2} \right) \right) ; \lambda \geq 0 , \\
&= \hat{N} \left(1 + \left(\frac{\Delta}{2t} - \frac{\Sigma}{2\Delta} \right) \log \left(\frac{m_a^2}{m_b^2} \right) \right. \\
&\quad \left. - \frac{\tilde{\lambda}}{t} \left(\arctan \left(\frac{t - \Delta}{\tilde{\lambda}} \right) - \arctan \left(\frac{-t - \Delta}{\tilde{\lambda}} \right) \right) \right) ; \lambda < 0 .
\end{aligned} \tag{E.6}$$

with:

$$\Sigma := m_a^2 + m_b^2 ; \quad \Delta := m_b^2 - m_a^2 .$$

$$\tilde{\lambda} := \sqrt{|\lambda|} ; \quad \lambda := (t - (m_b - m_a)^2)(t - (m_a + m_b)^2) .$$

References

- [1] L.-F. Li and H. Pagels, Phys. Rev. Lett. **26**, 1204 (1971).
- [2] C. W. Bernard, T. Draper, A. Soni, H. D. Politzer, and M. B. Wise, Phys. Rev. **D32**, 2343 (1985).
- [3] J. Bijnens, G. Colangelo, G. Ecker, J. Gasser, and M. E. Sainio, Phys. Lett. **B374**, 210 (1996), hep-ph/9511397.
- [4] G. Amoros, J. Bijnens, and P. Talavera, Nucl. Phys. **B568**, 319 (2000), hep-ph/9907264.
- [5] J. Bijnens and P. Talavera, Nucl. Phys. **B669**, 341 (2003), hep-ph/0303103.
- [6] J. Bijnens, G. Colangelo, and G. Ecker, Phys. Lett. **B441**, 437 (1998), hep-ph/9808421.
- [7] J. Laiho and A. Soni, Phys. Rev. **D65**, 114020 (2002), hep-ph/0203106.
- [8] M. Buchler, Eur. Phys. J. **C44**, 111 (2005), hep-ph/0504180.
- [9] G. Ecker, Prog. Part. Nucl. Phys. **35**, 1 (1995), hep-ph/9501357.
- [10] G. Colangelo and G. Isidori, (2000), hep-ph/0101264.
- [11] J. Kambor, J. Missimer, and D. Wyler, Nucl. Phys. **B346**, 17 (1990).
- [12] G. Ecker, J. Kambor, and D. Wyler, Nucl. Phys. **B394**, 101 (1993).

- [13] CP-PACS, J. I. Noaki *et al.*, Phys. Rev. **D68**, 014501 (2003), hep-lat/0108013.
- [14] RBC, T. Blum *et al.*, Phys. Rev. **D68**, 114506 (2003), hep-lat/0110075.
- [15] J. Bijnens, Phys. Lett. **B152**, 226 (1985).
- [16] M. Soldate and R. Sundrum, Nucl. Phys. **B340**, 1 (1990).
- [17] A. I. Davydychev and J. B. Tausk, Nucl. Phys. **B397**, 123 (1993).
- [18] G. Amoros, J. Bijnens, and P. Talavera, Nucl. Phys. **B602**, 87 (2001), hep-ph/0101127.
- [19] R. Unterdorfer and G. Ecker, (2005), hep-ph/0507173.
- [20] M. Buchler, G. Colangelo, J. Kambor, and F. Orellana, Phys. Lett. **B521**, 22 (2001), hep-ph/0102287.
- [21] J. A. M. Vermaseren, (2000), math-ph/0010025.
- [22] A. Nehme and P. Talavera, Phys. Rev. **D65**, 054023 (2002), hep-ph/0107299.
- [23] J. Gasser and H. Leutwyler, Nucl. Phys. **B250**, 465 (1985).
- [24] J. Bijnens, G. Colangelo, and G. Ecker, Annals Phys. **280**, 100 (2000), hep-ph/9907333.